

# PARTIALLY SPECIFIED SPATIAL AUTOREGRESSIVE MODEL WITH ARTIFICIAL NEURAL NETWORK

Wenqian Wang

Beth Andrews

Department of Statistics

Northwestern University

## Abstract

Spatial autoregressive model, introduced by Cliff and Ord in 1970s[11] has been widely applied in many areas of science and econometrics such as regional economics, public finance, political sciences, agricultural economics, social sciences, economic development, environmental studies and transportation analyses. Based on the classical space autoregressive models, Su and Jin [31] proposed a semi-parametric model named as partially specified spatial autoregressive model (PSAR) to allow for more flexibility in modeling. This paper extends an artificial neural network model to a partially specified space autoregressive model and proposes maximum likelihood estimators instead of quasi-maximum likelihood estimates. We establish the consistency and asymptotic normality of the estimators in this model. These results are obtained under some standard conditions in spatial models as well as neural network models. To illustrate, we investigate the quality of the normal approximation for finite samples by means of numerical simulation studies with three common choices of error distributions (standard normal, student-t distribution and the Laplace distribution) and apply our proposed model to a soil-water tension problem[9] and a criminal study in Chicago.

---

## 1 Introduction

One commonly used assumption in regression analysis is that observations are uncorrelated, but this assumption is sometimes impossible to be defended in the analysis of spatial data when one observation may be related to neighboring entities. The nature of the covariance among observations may not be known precisely and researchers have been dedicated for years to building appropriate models to describe such correlation. The collection of techniques to investigate properties in the spatial models is considered to have begun in the domain of spatial econometrics first proposed by Paelinck in the early 1970s [24]. Later, the books by Cliff and Ord [11], Anselin [3] and Cressie [9] detailed research results related to spatial autocorrelation, purely spatial dependence as well as cross-sectional and/or panel data.

So why has estimating the spatial correlation drawn so much attention? In some applications estimating the spatial structure of the dependence may be a subject of interest or provide a key insight; in other contexts, it may be regarded as serial correlations. However, in either case, inappropriate treatment of data with spatial dependence can lead to inefficient or biased and inconsistent estimates. These consequences may result in misleading conclusions in the analysis of real world problems. Therefore, it is important to describe spatial dependence; some standard parametric models are spatial autoregressive models (SAR), spatial error models (SEM) and spatial Durbin models (LeSage, R. Pace, [18]). According to the spatial autoregressive model, values of the dependent variable depend on observations in neighboring regions. The SAR model has been widely discussed in the literature, and researchers have proposed various parameter estimation techniques such as the method of maximum likelihood by Ord [23] and Smirnov and Anselin [30], the method of moments by Kelejian and Prucha [14, 16, 15] and the method of quasi-maximum likelihood estimation by Lee [17].

In a SAR model with covariates, the observations are modeled by a weighted average of neighboring observations with weights determined by the distance between them:

$$y_s = \rho \sum_{i=1}^n w_{si} y_i + x_s' \beta + \varepsilon_s \quad s = 1, 2, \dots, n$$

where  $y_s$  denotes the observation and  $x_s$  denotes the value of a  $p$  dimensional independent variable at location  $s \in \{1, 2, \dots, n\}$ .  $w_{ij}$  is the  $(i, j)$  entry of a  $n \times n$  weight matrix  $\mathbf{W}$ ; it contains a set of nonnegative weights which represent the degree of interaction between units  $i$  and  $j$ . By convention,

---

we always set  $w_{ii} = 0$ . The random disturbances  $\{\varepsilon_s\}_{s=1}^n$  are uncorrelated with zero means and equal variances; usually we take them to be normally distributed. The model has parameter vector  $\theta = (\rho, \beta')$ . However, parametric models are vulnerable to the preciseness of model specification: a misspecified model can draw misleading inferences. Whereas a nonparametric model is more robust even though it sacrifices the precision. In this sense, to combine the advantages of these two models, we consider a semi-parametric model in the spatial context. The suggested model, a partially specified spatial autoregressive model (PSAR) [31], is defined as follows:

$$y_s = \rho \sum_{i=1}^n w_{si} y_i + x_s' \beta + g(z_s) + \varepsilon_s \quad s = 1, 2, \dots, n \quad (1)$$

where  $g(\cdot)$  is an unknown function and  $z_s$  denotes a  $q$  dimension vector of explanatory variables at location  $s$ . This PSAR model has a more flexible functional form than the ordinary spatial autoregressive model. Methods of parameter estimation for the PSAR model include profile quasi-maximum likelihood estimation by Su and Jin [31] and a sieve method by Zhang [37]. In Su and Jin [31], they used profile quasi-maximum likelihood estimators for independent and identically distributed errors and gave an asymptotic analysis using local polynomials. This method showed its advantage in dimension reduction when maximizing concentrated likelihood function with respect to one parameter  $\rho$  but involved in two-stage maximization if we wanted to obtain other parameter estimators such as  $\beta$ 's. However, in Zhang [37], they were using a sieve method (Ai, Chen [1]) to approximate the nonparametric function. They applied a sequence of known basis functions to approximate  $g(\cdot)$  in equation (1), and used the two-stage least squares estimation with some instrumental variables to obtain consistent estimators for the PSAR model.

Both methods use Gaussian likelihood techniques and do not specify distributions of the random disturbances  $\varepsilon_s$ . But normality is unreasonable in many cases when we observe errors with heavy tails or abnormal patterns. If this is the case, maximum likelihood estimation can be more efficient than Gaussian-based quasi-maximum likelihood estimation. Another difference is that we are using neural network models to estimate the nonlinear function  $g(\cdot)$  whereas Su and Jin [31] applied a finite order of local polynomials about some explanatory variables and Zhang [37] used a linear combination of a sequence of known functions to estimate  $g(\cdot)$ .

The purpose of this paper is to extend an autoregressive artificial neural network (Medeiros, Teräsvirta, Rech [21]) developed in the context of time series data to a partially specified spatial autoregressive model and we regard the artificial neural network part as a nonlinear statistical

---

component to approximate the nonparametric function  $g(\cdot)$  in the PSAR model (1). The use of an ANN (Artificial Neural Network) model is motivated by mathematical results showing that under mild conditions, a relatively simple ANN model is competent in approximating any Borel-measurable function to any given degree of accuracy (see for example Hornik *et al.* [12], Gallant and White [10]). Under this theoretical foundation, we would expect our model to perform well when modeling nonparametric components in spatial contexts. Another improvement is that, in our model, the random error is independent and identically distributed but does not necessarily follow a normal distribution. We derive parameter estimates by maximizing the corresponding likelihood function and discuss the asymptotic properties of our estimators under conditions that the spatial weight matrix is nonsingular and the log likelihood function has some dominated function with a finite mean.

In Sections 2 and 3, our model PSAR-ANN is given and a likelihood function for corresponding parameters is derived. In Sections 4 and 5, we discuss model identification and establish consistency and asymptotic normality for MLEs of model parameters. In section 6, we describe numerical simulation studies to investigate how well the behavior of estimators for finite samples matches the limiting theory, i.e., the quality of the normal approximation. The PSAR-ANN model is fit to two real world datasets soil-water tension and criminal events in Chicago.

## 2 Model Specification

The main focus of this paper is to approximate the nonparametric function  $g(\cdot)$  in the partially specified spatial autoregressive model (1) by an artificial neural network model. The model in matrix form is defined as

$$\mathbf{Y} = \mathbf{X}\boldsymbol{\beta} + \rho\mathbf{W}\mathbf{Y} + \boldsymbol{\Lambda}\mathbf{F}(\mathbf{X}\boldsymbol{\gamma}) + \boldsymbol{\varepsilon} \quad (2)$$

where  $\mathbf{Y} = \{y_s\}_{s=1}^n$  contains observations of the dependent variable at  $n$  locations. The independent variable matrix  $\mathbf{X} = (\mathbf{x}_1, \mathbf{x}_2, \dots, \mathbf{x}_n)' \in \mathbb{R}^{n \times q}$  contains values of exogenous regressors for the  $n$  regions, where for each region,  $\mathbf{x}_s = (x_{s1}, \dots, x_{sq})'$ ,  $s = 1, 2, \dots, n$  is a  $q$  dimension vector.  $\boldsymbol{\varepsilon} = (\varepsilon_1, \varepsilon_2, \dots, \varepsilon_n)'$  denotes a vector of  $n$  independent identically distributed random noises with density function  $f$ , mean 0 and variance  $\sigma^2$ .

Parameter  $\boldsymbol{\beta} = (\beta_1, \dots, \beta_q)' \in \mathbb{R}^q$  and scalar  $\rho$ , the spatial autoregressive parameter, are as-

---

sumed to be the same over all regions.  $\mathbf{W} = \{w_{ij}\} \in \mathbb{R}^{n \times n}$  denotes a spatial weight matrix (we discuss this later in detail) which characterizes the connections between regions.

The artificial neural network component (Medeiros *et al.* [21]) is  $\mathbf{\Lambda F}(\mathbf{X}\boldsymbol{\gamma})$ .

$$\begin{aligned}\mathbf{F}(\mathbf{X}\boldsymbol{\gamma}) &= (F(\mathbf{x}'_1\boldsymbol{\gamma}_1), F(\mathbf{x}'_1\boldsymbol{\gamma}_2), \dots, F(\mathbf{x}'_1\boldsymbol{\gamma}_h), \\ &\quad F(\mathbf{x}'_2\boldsymbol{\gamma}_1), F(\mathbf{x}'_2\boldsymbol{\gamma}_2), \dots, F(\mathbf{x}'_2\boldsymbol{\gamma}_h), \\ &\quad \dots, \\ &\quad F(\mathbf{x}'_n\boldsymbol{\gamma}_1), \dots, F(\mathbf{x}'_n\boldsymbol{\gamma}_h))' \in \mathbb{R}^{nh}\end{aligned}$$

This vector represents a single layer neural network with  $h$  neurons for every location. The value of  $h$  is determined by researchers and can be selected by comparing AIC/BIC. Under this setting, the parameter matrix  $\boldsymbol{\gamma} = (\boldsymbol{\gamma}_1, \boldsymbol{\gamma}_2, \dots, \boldsymbol{\gamma}_h)' \in \mathbb{R}^{h \times q}$ ,  $\boldsymbol{\gamma}_i = (\gamma_{i1}, \dots, \gamma_{iq})' \in \mathbb{R}^q$ ,  $i = 1, 2, \dots, h$ , contains all the weights in a neural network model.  $F(\cdot)$  is called the activation function and here we assign it to be the logistic function. For given information  $\mathbf{x}_s$  at region  $s$ , the corresponding output of  $i$ th neuron in a single layer neural network is

$$F(\mathbf{x}'_s\boldsymbol{\gamma}_i) = (1 + e^{-\mathbf{x}'_s\boldsymbol{\gamma}_i})^{-1}, \quad s = 1, 2, \dots, n, i = 1, 2, \dots, h$$

Parameter vector  $\boldsymbol{\lambda} = (\lambda_1, \lambda_2, \dots, \lambda_h)'$  denotes weights for  $h$  neurons. In formula (2),  $\mathbf{\Lambda} = \text{diag}(\boldsymbol{\lambda}', \boldsymbol{\lambda}', \dots, \boldsymbol{\lambda}') \in \mathbb{R}^{n \times nh}$ . So  $\mathbf{\Lambda F}(\mathbf{X}\boldsymbol{\gamma}) =$

$$\begin{pmatrix} \lambda_1 & \dots & \lambda_h & 0 & 0 & 0 & \dots & 0 & 0 \\ 0 & \dots & 0 & \lambda_1 & \dots & \lambda_h & 0 & \dots & 0 \\ \vdots & \vdots & \vdots & \ddots & \ddots & \ddots & \vdots & \vdots & \vdots \\ 0 & 0 & 0 & 0 & \dots & 0 & \lambda_1 & \dots & \lambda_h \end{pmatrix} \begin{pmatrix} F(\mathbf{x}'_1\boldsymbol{\gamma}_1) \\ F(\mathbf{x}'_1\boldsymbol{\gamma}_2) \\ \vdots \\ F(\mathbf{x}'_1\boldsymbol{\gamma}_h) \\ F(\mathbf{x}'_2\boldsymbol{\gamma}_1) \\ F(\mathbf{x}'_2\boldsymbol{\gamma}_2) \\ \vdots \\ F(\mathbf{x}'_2\boldsymbol{\gamma}_h) \\ \vdots \\ F(\mathbf{x}'_n\boldsymbol{\gamma}_1) \\ F(\mathbf{x}'_n\boldsymbol{\gamma}_2) \\ \vdots \\ F(\mathbf{x}'_n\boldsymbol{\gamma}_h) \end{pmatrix} = \begin{pmatrix} \sum_{i=1}^h \lambda_i F(\mathbf{x}'_1\boldsymbol{\gamma}_i) \\ \sum_{i=1}^h \lambda_i F(\mathbf{x}'_2\boldsymbol{\gamma}_i) \\ \vdots \\ \sum_{i=1}^h \lambda_i F(\mathbf{x}'_n\boldsymbol{\gamma}_i) \end{pmatrix} \in \mathbb{R}^n$$

One important element in the model (2) is the spatial weight matrix  $\mathbf{W}$ . The spatial weights depend on the definition of a neighborhood set for each observation. In our applications we begin by using a square symmetric  $n \times n$  matrix with  $(i, j)$  element equal to 1 if regions  $i$  and  $j$  are neighbors (possible to be correlated) and  $w_{ij} = 0$  otherwise. The diagonal elements of the spatial neighbors matrix are set to zero. Then we row standardize the weight matrix, so the nonzero weights are scaled so that the weights in each row sum up to 1. In convention, people usually use

---

the row standardized weight matrices because row standardization creates proportional weights in cases where features have an unequal number of neighbors; also this normalized matrix has nice properties in the range of eigenvalues (this will be mentioned later). As LeSage [19] suggests, there is a vast number of ways to construct such a matrix. We discuss some commonly used methods in lattice cases and non-lattice cases. In a lattice case shown in the following Figure 1, we have 9 locations and we label them as  $1, 2, \dots, 9$  at left corners in each cell. Suppose  $i$  is the target location and  $j$  identifies the neighborhood of  $i$ .

- Rook Contiguity (Fig 1 (a)): two regions are neighbors if they share (part of) a common edge (on any side)
- Bishop Continuity (Fig 1 (b)): two regions are spatial neighbors if they share a common vertex (or a point)
- Queen Contiguity (Fig 1 (c)): this is the union of Rook and Bishop contiguity. Two regions are neighbors in this sense if they share any common edge or vertex

Figure 1 consists of three 3x3 grids labeled (a), (b), and (c). Grid (a) shows Rook Contiguity where cells (1,2), (2,1), (2,3), and (3,2) are neighbors of cell (2,2). Grid (b) shows Bishop Contiguity where cells (1,1), (1,3), (3,1), and (3,3) are neighbors of cell (2,2). Grid (c) shows Queen Contiguity where all 8 cells in the 3x3 grid are neighbors of cell (2,2).

	$j$	
1	2	3
$j$	$i$	$j$

(a)

$j$		$j$
1	2	3
	$i$	

(b)

$j$	$j$	$j$
1	2	3
$j$	$i$	$j$
4	5	6
$j$		$j$
7	8	9

(c)

**Figure 1:** Examples of Rook (a), Bishop (b) and Queen Contiguity (c)

In practice, usually we may not always have a problem in a lattice. So an analog of an edge and a vertex is called “snap distance” such that any border larger than this “snap distance” will be regarded as an edge or otherwise an vertex. So the Queen contiguity may be interpreted as that two regions are neighbors as long as they are connected no matter how short the common border is. Under the Queen criterion, for example, based on the example illustrated in Figure (1(c)), a  $9 \times 9$  weight matrix for nine locations is shown below.

$$\begin{pmatrix} 0 & 1 & 0 & 1 & 1 & 0 & 0 & 0 & 0 \\ 1 & 0 & 1 & 1 & 1 & 1 & 0 & 0 & 0 \\ 0 & 1 & 0 & 0 & 1 & 1 & 0 & 0 & 0 \\ 1 & 1 & 0 & 0 & 1 & 0 & 1 & 1 & 0 \\ 1 & 1 & 1 & 1 & 0 & 1 & 1 & 1 & 1 \\ 0 & 1 & 1 & 0 & 1 & 0 & 0 & 1 & 1 \\ 0 & 0 & 0 & 1 & 1 & 0 & 0 & 1 & 0 \\ 0 & 0 & 0 & 1 & 1 & 1 & 0 & 1 & 0 \\ 0 & 0 & 0 & 0 & 1 & 1 & 0 & 1 & 0 \end{pmatrix}$$

However, in a non-lattice case when units, such as cities, are only points, this neighborhood definition does not work because all units/points do not share any common edge or vertex. So a distance based method is utilized to deal with such point case. Denote  $d_{ij} \equiv d(i, j)$  as the distance between two units/points  $i$  and  $j$ , then some commonly used ways to define neighborhoods are

- Minimum Distance Neighbors:

A neighbor  $j$  of unit  $i$  satisfies that their distance  $d_{ij} \in (0, \max_{i \in \{1, \dots, n\}} \min_{i \neq j} d(i, j)]$ . This method controls that every unit has at least one neighbor but usually includes a large number of irrelevant connections.

- K-nearest Neighbors:

Neighbors of  $i$  are restricted by the user-defined parameter  $K$ . A unit  $j$  is a neighbor of  $i$  if  $j \in N_K(i)$ , where  $N_K(i)$  defines the K-nearest neighbors of  $i$ . This method also guarantees that there is no neighborless unit and has less noise than the Minimum Distance Neighbors. However, the user-choice parameter  $K$  may not reflect the true level of connectedness or isolation between points.

- Sphere of Influence Neighbors:

For each point  $i \in S = \{1, \dots, n\}$ ,  $r_i = \min_{k \neq i} d(i, k)$  and denote  $C_i$  as a circle of radius  $r_i$  centered at  $i$ . Units  $i$  and  $j$  are neighborhoods whenever  $C_i$  and  $C_j$  intersect in exactly two points. This graph-based method improves the K-nearest Neighbors in a way that relatively long links are avoided and the number of connections per unit is variable. This method works well even in an irregularly located areal entities and precludes the intervention of user-defined parameter  $K$  in the previous method (See Figure 2).

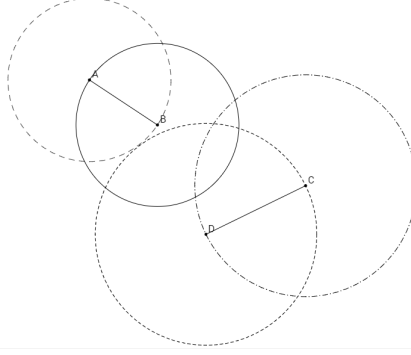


**Figure 2: Sphere of Influence Graph:** A,B,C,D represent four units. Where the circles around each city overlap in at least two points, the cities can be considered neighbors. In the current example, A is a neighbor of only B, B is a neighbor to all, C is a neighbor of B and D, D is a neighbor of B and C but not A.

According to Figure 2, the weight matrix for A, B, C and D is:

$$\begin{pmatrix} 0 & 1 & 0 & 0 \\ 1 & 0 & 1 & 1 \\ 0 & 1 & 0 & 1 \\ 0 & 1 & 1 & 0 \end{pmatrix}$$

To write our model (2) more explicitly, for each location  $s$ ,  $s = 1, 2, \dots, n$

$$y_s = \mathbf{x}'_s \boldsymbol{\beta} + \rho \sum_{i=1}^n w_{si} y_i + \sum_{i=1}^h \lambda_i F(\mathbf{x}'_s \boldsymbol{\gamma}_i) + \varepsilon_s \quad (3)$$

The term  $\sum_{i=1}^h \lambda_i F(\mathbf{x}'_s \boldsymbol{\gamma}_i)$ , a linear combination of logistic functions with weights  $\lambda_i, i = 1, 2, \dots, h$ , forms a hidden layer of this neural network with  $h$  neurons (Medeiros, Teräsvirta, Rech [21]). This neural network helps discover nonlinear relationship between the response variable and its covariates.

### 3 Likelihood Function

Rewriting the function in (2), we have,

$$(\mathbf{I}_n - \rho \mathbf{W}) \mathbf{Y} - \mathbf{X} \boldsymbol{\beta} - \mathbf{\Lambda} \mathbf{F}(\mathbf{X} \boldsymbol{\gamma}) = \boldsymbol{\varepsilon} \quad (4)$$

where  $\mathbf{I}_n$  is an  $n \times n$  identity matrix. We denote  $\boldsymbol{\theta} = (\beta_1, \dots, \beta_q, \rho, \lambda_1, \dots, \lambda_h, \boldsymbol{\gamma}'_1, \dots, \boldsymbol{\gamma}'_h)' \in \mathbb{R}^{(q+1)(h+1)}$  with true value  $\boldsymbol{\theta}_0$ . In the following, we denote  $\mathbf{S}(\rho) = \mathbf{I}_n - \rho \mathbf{W}$ , and  $\mathbf{S}_0 = \mathbf{I}_n - \rho_0 \mathbf{W}$ , where  $\rho_0$  is the true value for the spatial correlation coefficient.

For the analysis of identification and estimation of this spatial autoregressive model (2), we adopt the following assumptions:

---

**Assumption 1.** The spatial correlation coefficient  $\rho$  satisfies

$$\rho \in (-1/\tau, 1\tau)$$

where  $\tau = \max\{|\tau_1|, |\tau_2|, \dots, |\tau_n|\}$ ,  $\tau_1, \dots, \tau_n$  are eigenvalues of spatial weight matrix  $\mathbf{W}$ .

This assumption defines the parameter space for  $\rho$  as an interval around zero such that  $\mathbf{I}_n - \rho\mathbf{W}$  is strictly diagonally dominant and by the Levy-Desplanques theorem it follows that  $\mathbf{S}(\rho)$  is non-singular ( Lévy, Desplanques (1881-1886)) for any values  $\rho$  in that interval. Note that the diagonal entries in  $\mathbf{S}(\rho)$  are all 1 (because  $w_{ii} = 0$ ). Using the Gershgorin circle theorem it can be proved that  $\mathbf{S}(\rho)$  is also positive semidefinite. It can be shown that for a row-normalized matrix  $\mathbf{W}$ ,  $-1 < \rho < 1$ . Using the  $9 \times 9$  non-standardized weight matrix constructed under Queen's criterion in the previous section, the interval for  $\lambda$  is  $(-0.207, 0.207)$  whereas the row standardized weight matrix has the interval  $(-1, 1)$ .

**Assumption 2.** The error terms  $\varepsilon_s$ ,  $s = 1, 2, \dots, n$  are independent and identical distributed with zero mean and constant variance  $\sigma^2 = 1$ .

The assumption  $\sigma^2 = 1$  is made so that all model parameters are identifiable.

**Assumption 3.** The  $(q+1)(h+1)$  parameter vector  $\boldsymbol{\theta} = (\boldsymbol{\beta}', \rho, \boldsymbol{\lambda}', \boldsymbol{\gamma}'_1, \dots, \boldsymbol{\gamma}'_h)' \in \Theta$ , where  $\Theta$  is a subset of the  $(q+1)(h+1)$  dimensional Euclidean space,  $\mathbb{R}^{(q+1)(h+1)}$ .  $\Theta$  is a closed and bounded compact set and contains the true value of  $\boldsymbol{\theta}$ , denoted by  $\boldsymbol{\theta}_0$ , as an interior point.

Assuming that errors  $\{\varepsilon_s\}_{s=1}^n$  have an identical density function  $f$ , to derive the likelihood function of  $\boldsymbol{\theta}$ , it is necessary to introduce the Jacobian coefficient which allows us to derive the joint distribution of  $\mathbf{Y} = \{y_s\}_{s=1}^n$  from that of  $\{\varepsilon_s\}_{s=1}^n$ , through equation (4):

$$J = \det(\partial \mathbf{Y} / \partial \varepsilon) = |\mathbf{S}(\rho)| \quad (5)$$

Hence, based on a joint distribution for the vector of independent errors  $\{\varepsilon_s\}_{s=1}^n$ , and using (5) the log-likelihood function for the joint vector of observations,  $\boldsymbol{\theta}$ , is given by (Anselin, p.63 [3])

$$\begin{aligned} \mathcal{L}_n(\boldsymbol{\theta}) &= \ln |\mathbf{S}(\rho)| + \sum_{s=1}^n \ln f(\varepsilon_s(\boldsymbol{\theta})) \\ \varepsilon_s(\boldsymbol{\theta}) &= y_s - \mathbf{x}'_s \boldsymbol{\beta} - \rho \sum_{i=1}^n w_{si} y_i - \sum_{i=1}^h \lambda_i F(\mathbf{x}'_s \boldsymbol{\gamma}_i) \end{aligned} \quad (6)$$

In practice, the density function  $f$  could be chosen by looking at the distribution for observations and model residuals  $\varepsilon_s(\boldsymbol{\theta})$ . Common choices are normal distribution, t-distribution and Laplace

---

distribution. We examined these three distributions (with unit variances under Assumption 2) and the corresponding log-likelihood functions functions are given below.

When  $\varepsilon_s \sim N(0, 1)$ ,

$$f(\varepsilon_s) = \frac{1}{\sqrt{2\pi}} \exp\left(-\frac{\varepsilon_s^2}{2}\right)$$

$$\mathcal{L}_n(\boldsymbol{\theta}) = \ln |\mathbf{S}(\rho)| - \frac{n}{2} \ln(2\pi) - \frac{1}{2} \sum_{s=1}^n \varepsilon_s^2(\boldsymbol{\theta})$$

When  $\varepsilon_s \sim t$ -distribution with degree of freedom  $\nu$  ( $\nu > 2$ , known), we use the rescaled t density which is symmetric about zero and has variance 1:

$$f(\varepsilon_s) = \sqrt{\frac{\nu}{\nu-2}} \frac{\Gamma[\frac{1}{2}(\nu+1)]}{\sqrt{\nu\pi} \Gamma(\frac{1}{2}\nu)} \cdot \left(1 + \frac{\varepsilon_s^2}{\nu-2}\right)^{-\frac{1+\nu}{2}}$$

$$\mathcal{L}_n(\boldsymbol{\theta}) = \ln |\mathbf{S}(\rho)| - \frac{n}{2} \ln(\nu-2)\pi + n \ln \frac{\Gamma[\frac{1}{2}(\nu+1)]}{\Gamma(\frac{1}{2}\nu)} - \frac{1+\nu}{2} \sum_{s=1}^n \ln \left(1 + \frac{\varepsilon_s^2(\boldsymbol{\theta})}{\nu-2}\right)$$

When  $\varepsilon_s \sim$  Laplace distribution with mean  $\mu = 0$  scale parameter  $b = \sqrt{2}/2$ ,

$$f(\varepsilon_s) = \frac{1}{\sqrt{2}} \exp\left(-\sqrt{2}|\varepsilon_s|\right)$$

$$\mathcal{L}_n(\boldsymbol{\theta}) = \ln |\mathbf{S}(\rho)| - \frac{n}{2} \ln 2 - \sum_{s=1}^n \sqrt{2}|\varepsilon_s(\boldsymbol{\theta})|$$

In the following sections, we will discuss model identifiability and establish asymptotic properties for the maximum likelihood estimator  $\hat{\boldsymbol{\theta}}_{ML} = \arg \max_{\boldsymbol{\theta} \in \Theta} \mathcal{L}_n(\boldsymbol{\theta})$ .

## 4 Model Identification

We now investigate the conditions under which our proposed model is identified. By Rothenberg [28], a parameter  $\theta_0 \in \Theta$  is *globally identified* if there is no other  $\theta$  in  $\Theta$  that observationally equivalent to  $\theta_0$  such that  $f(y, \theta) = f(y, \theta_0)$ ; or the parameter  $\theta_0$  is *locally identified* if there is no such  $\theta$  in an open neighborhood of  $\theta_0$  in  $\Theta$ . The model (3), in principle, is neither globally nor locally identified and the lack of identification of Neural Network models has been discussed in many papers (Hwang and Ding[13]; Medeiros *et al.* [21]). Here we extend the discussion to our proposed PSAR model. Three characteristics imply non-identification of our model: (a) the interchangeable property: the value in the likelihood function may remain unchanged if we permute the hidden units. For a model with  $h$  neurons, this will result in  $h!$  different models that are indistinguishable from each other and have equal local maximums of the log-likelihood function; (b) the “symmetry” property: for a logistic function,  $F(x) = 1 - F(-x)$  allows two equivalent parametrization for each

---

hidden units; (c) the reducible property: the presence of irrelevant neurons in model (3) happens when  $\lambda_i = 0$  for at least one  $i$  and parameters  $\gamma_i$  remain unidentified. Conversely, if  $\gamma_{ij} = \mathbf{0}$ ,  $j \neq 0$ ,  $\gamma_{i0}$  and  $\lambda_i$  can take any value without affecting the value of likelihood functions.

The problem of interchangeability (as mentioned in (a)) can be solved by imposing the following restriction, as in Medeiros *et al.* [21]:

**Restriction 1.** *parameters  $\gamma_{10}, \gamma_{20}, \dots, \gamma_{h0}, \lambda_1, \dots, \lambda_h$  are restricted such that:  $\gamma_{10} \leq \gamma_{20} \leq \dots \leq \gamma_{h0}$  or  $\lambda_1 \geq \dots \geq \lambda_h$ .*

And to tackle (b) and (c), we can apply another restriction:

**Restriction 2.** *The parameters  $\lambda_i$  and  $\gamma_{i1}$  should satisfy:*

- (1)  $\lambda_i \neq 0$ ,  $\forall i \in \{1, 2, \dots, M\}$ ; and
- (2)  $\gamma_{i1} > 0$ ,  $\forall i \in \{1, 2, \dots, M\}$ .

To guarantee the non-singularity of model matrices and the uniqueness of parameters, we impose the following basic assumption:

**Assumption 4.** The independent variable matrix  $\mathbf{X} \in \mathbf{R}^{n \times (q)}$  has full rank, i.e.,  $\text{rank}(\mathbf{X}) = q$ .

And furthermore, the true parameter vector  $\boldsymbol{\theta}_0$  satisfies Restrictions 1-2.

**Lemma 1.** Under the Assumptions 1-4, this partially specified spatial autoregressive model (3) is globally identified.

## 5 Asymptotic Results

### 5.1 Preliminary

Denote the true parameter vector as  $\boldsymbol{\theta}_0$  and the solution which maximizes the log-likelihood function (6) as  $\hat{\boldsymbol{\theta}}_n$ . Hence,  $\hat{\boldsymbol{\theta}}_n$  should satisfy

$$\hat{\boldsymbol{\theta}}_n \equiv \arg \max_{\boldsymbol{\theta} \in \Theta} \mathcal{L}_n(\boldsymbol{\theta}),$$

$$\mathcal{L}_n(\boldsymbol{\theta}) = \ln |\mathbf{S}(\rho)| + \sum_{s=1}^n \ln f(y_s - \mathbf{x}'_s \boldsymbol{\beta} - \rho \sum_{i=1}^n w_{si} y_i - \sum_{i=1}^h \lambda_i F(\mathbf{x}'_s \boldsymbol{\gamma}_i))$$

Suppose we have a  $n_1 \times n_2$  lattice where the total number of sampling units is large enough and we consider asymptotic properties of  $\hat{\boldsymbol{\theta}}_n$  when  $n = n_1 n_2 \rightarrow \infty$ . For notation simplicity, we denote  $z_s = (\mathbf{x}'_s, y_s, \sum_{i=1}^n w_{si} y_i)$ , where  $\sum_{i=1}^n w_{si} y_i$  is a weighted sum of the neighborhood observations of location  $s$ . So the log likelihood (6) can be regarded as a function of  $\boldsymbol{\theta}$  given  $\{z_s\}_{s=1}^n$ .

In a spatial context, we should notice that the functional form of  $y_s$  is not identical for all the locations due to values of the weights  $\{w_{si}\}_{i=1}^n$ . For example, in a lattice, units at edges, vertexes or in the interior have different density functions due to different neighborhood structures (Figure 3). Denote  $\mathcal{N}_s$  as a neighborhood set for location  $s$ . For an interior point (Figure 3(c)), its neighborhood set  $\mathcal{N}_s$  contains eight neighbors where  $w_{sj} = 1/8$  if  $j \in \mathcal{N}_s$  otherwise  $w_{sj} = 0$ , for  $j = 1, 2, \dots, n$ . However, an edge point (Figure 3(b)) has five neighboring units with  $w_{sj} = 1/5$  for  $j \in \mathcal{N}_s$  and the weight of a vertex neighborhood is  $1/3$  because a vertex unit has only three neighbors. This is known as an edge effect in spatial problems.

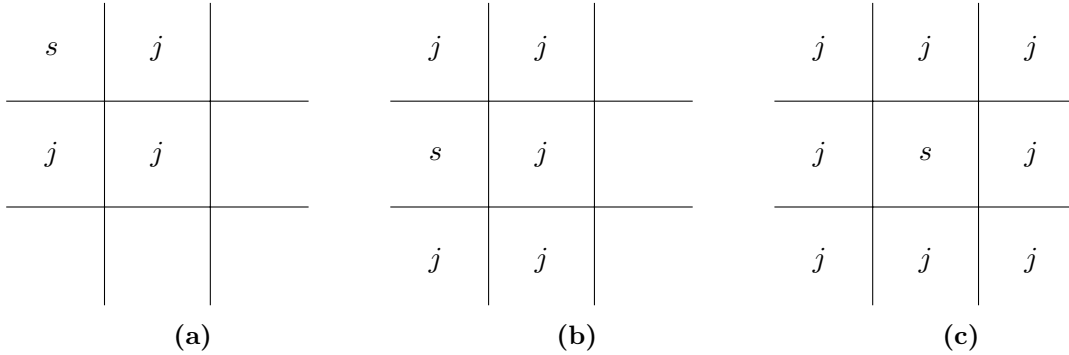


**Figure 3:** Vertex (a), Edge (b) and Interior Points (c) Neighborhood Structures:  $s$  is the target location and  $j$  represents the neighborhood of  $s$

To deal with this, define a set  $\mathcal{S}$  containing  $(n_1 - 2)(n_2 - 2)$  interior locations and a set  $\mathcal{M}$  containing the  $2(n_1 + n_2) - 4$  boundary locations. Then  $\mathcal{L}_n(\boldsymbol{\theta})$  can be split into a sum of two parts (interior and boundary parts):

$$\begin{aligned} \mathcal{L}_n(\boldsymbol{\theta}) &= \sum_{s \in \mathcal{M}} l(\boldsymbol{\theta}|z_s) + \sum_{s \in \mathcal{S}} l(\boldsymbol{\theta}|z_s) \\ l(\boldsymbol{\theta}|z_s) &= n^{-1} \ln |\mathbf{S}(\rho)| + \ln f(y_s - \mathbf{x}'_s \boldsymbol{\beta} - \rho \sum_{i=1}^n w_{si} y_i - \sum_{i=1}^h \lambda_i F(\mathbf{x}'_s \boldsymbol{\gamma}_i)) \end{aligned}$$

In order to establish the asymptotic properties of parameter estimate  $\hat{\boldsymbol{\theta}}_n$ , we propose a modified maximum likelihood estimator (similar modifications to reduce edge effects in Yao and Brockwell [36]): given that  $\lim_{n_1, n_2 \rightarrow \infty} \frac{2(n_1 + n_2) - 4}{n_1 n_2} = 0$  and  $\ln f(\cdot) < \infty$ ,  $n^{-1} \sum_{s \in \mathcal{M}} l(\boldsymbol{\theta}|z_s)$  vanishes as  $n$  tends to infinity. Therefore,

$$\begin{aligned} \lim_{n \rightarrow \infty} n^{-1} \mathcal{L}_n(\boldsymbol{\theta}) &= \lim_{n_1, n_2 \rightarrow \infty} (n_1 n_2)^{-1} \left( \sum_{s \in \mathcal{M}} l_s(\boldsymbol{\theta}|z_s) + \sum_{s \in \mathcal{S}} l_s(\boldsymbol{\theta}|z_s) \right) \\ &= \lim_{n_1, n_2 \rightarrow \infty} (n_1 n_2)^{-1} \sum_{s \in \mathcal{S}} l(\boldsymbol{\theta}|z_s) \end{aligned}$$

The condition  $\ln f(\cdot) < \infty$  is generally true and holds for the three densities mentioned before. In this equation, every location  $s \in \mathcal{S}$  has eight neighboring units under the queen criterion with the

weights  $w_{sj} = 1/8$  when  $j \in \mathcal{N}_s$ . Hence for an interior unit  $s$ ,  $\sum_{i=1}^n w_{si} y_i = \sum_{j \in \mathcal{N}_s} y_j / 8$ . And the log likelihood function  $\mathcal{L}_n(\boldsymbol{\theta})$  is approximately

$$\mathcal{L}_n(\boldsymbol{\theta}) \approx \sum_{s \in \mathcal{S}} l(\boldsymbol{\theta}|z_s) \quad \text{for large } n \quad (7)$$

And further the maximum likelihood estimator  $\hat{\boldsymbol{\theta}}_n$  approximately maximizes  $\sum_{s \in \mathcal{S}} l(\boldsymbol{\theta}|z_s)$ . Because division by  $n$  does not affect the maximizing problem, for large  $n$ ,

$$\hat{\boldsymbol{\theta}}_n \approx \arg \max_{\boldsymbol{\theta} \in \Theta} n^{-1} \sum_{s \in \mathcal{S}} l(\boldsymbol{\theta}|z_s)$$

## 5.2 Consistency Results

To establish the consistency of  $\hat{\boldsymbol{\theta}}_n$ , the heuristic insight is that because  $\hat{\boldsymbol{\theta}}_n$  approximately maximizes  $n^{-1} \sum_{s \in \mathcal{S}} l(\boldsymbol{\theta}|z_s)$  and because  $n^{-1} \sum_{s \in \mathcal{S}} l(\boldsymbol{\theta}|z_s)$  can generally be shown to tend to a real function  $\mathcal{L} : \Theta \rightarrow \mathbb{R}$  with maximizer  $\boldsymbol{\theta}_0$  as  $n \rightarrow \infty$  under mild conditions on the data generating process, then  $\hat{\boldsymbol{\theta}}_n$  should tend to  $\boldsymbol{\theta}_0$  almost surely. Before the formal proof of the consistency, we need the following assumptions on density function  $f(\cdot; \boldsymbol{\theta})$  satisfied (similar assumptions are made in White [35], Andrews, Davis and Breidt [2], Lii and Rosenblatt [20]).

### Assumption 5.

1. For all  $z \in \mathbb{R}$  and all  $\boldsymbol{\theta} = (\boldsymbol{\beta}', \rho, \boldsymbol{\lambda}', \boldsymbol{\gamma}'_1, \dots, \boldsymbol{\gamma}'_h)' \in \Theta$ ,  $f(z; \boldsymbol{\theta}) > 0$  and  $f(s; \boldsymbol{\theta})$  is twice continuously differentiable with respect to  $(z, \boldsymbol{\theta}')$ .
2. For all  $\boldsymbol{\theta}$  in some neighborhood of  $\boldsymbol{\theta}_0$ ,  $\int z f'(z; \boldsymbol{\theta}) dz = z f(z; \boldsymbol{\theta})|_{-\infty}^{\infty} - \int f(z; \boldsymbol{\theta}) dz = -1$ .
3.  $\int f''(z; \boldsymbol{\theta}_0) dz = f'(z; \boldsymbol{\theta}_0)|_{-\infty}^{\infty} = 0$ .
4.  $\int z^2 f''(z; \boldsymbol{\theta}_0) dz = z^2 f'(z; \boldsymbol{\theta}_0)|_{-\infty}^{\infty} - 2 \int z f'(z; \boldsymbol{\theta}) dz = 2$ .
5.  $1 < \int (f'(z; \boldsymbol{\theta}))^2 / f(z; \boldsymbol{\theta}) dz$ .
6.  $f(z; \boldsymbol{\theta})$  is equicontinuous on  $\mathbb{R} \times \Theta$ , i.e. given  $\varepsilon > 0$ , there is a  $\delta > 0$  such that for  $\|(z_1, \boldsymbol{\theta}_1) - (z_2, \boldsymbol{\theta}_2)\| < \delta$ ,  $|f(z_1; \boldsymbol{\theta}_1) - f(z_2; \boldsymbol{\theta}_2)| < \varepsilon$ .
7. For  $j, k = 1, \dots, (q+2)(h+1)$  and all  $\boldsymbol{\theta}$  in some neighborhood of  $\boldsymbol{\theta}_0$ ,  $f(s; \boldsymbol{\theta})$  is dominated by some function  $f_1(z)$  such that  $\int z^2 f_1(z) dz < \infty$ ; and  $z^2 \frac{(f'(z; \boldsymbol{\theta}))^2}{f^2(z; \boldsymbol{\theta})}$ ,  $z^2 \left| \frac{f''(z; \boldsymbol{\theta})}{f^2(z; \boldsymbol{\theta})} \right|$ ,

$\frac{|z|}{f(z;\boldsymbol{\theta})} \left| \frac{\partial}{\partial \boldsymbol{\theta}_j} f'(z;\boldsymbol{\theta}) \right|$ ,  $\frac{1}{f^2(z;\boldsymbol{\theta})} \left( \frac{\partial}{\partial \boldsymbol{\theta}_j} f(z;\boldsymbol{\theta}) \right)^2$ , and  $\frac{1}{f(z;\boldsymbol{\theta})} \left| \frac{\partial^2}{\partial \boldsymbol{\theta}_j \partial \boldsymbol{\theta}_k} f(z;\boldsymbol{\theta}) \right|$  are dominated by  $a_1 + a_2 |z|^{c_1}$ , where  $a_1, a_2, c_1$  are non-negative constants and  $\int |z|^{c_1} f_1(z) dz < \infty$ , and  $E f_1^{1+\delta}(z;\boldsymbol{\theta}) < \infty$  for some  $\delta > 0$ .

Discussed in Breidt, Davis, Lii and Rosenblatt [5] and Andrews, Davis and Breidt (p.1642-1645 [2]), these assumptions on the density  $f(\cdot)$  are satisfied in the t-distribution case when  $\nu > 2$  and the standard normal case. Although the Laplace distribution does not strictly satisfy the Assumption 5, since it is not everywhere differentiable, we believe the limiting results remain valid for parameter estimates.

As Newey [22] pointed out that a equicontinuity can often be obtained by a suitable redefinition of the data. So Assumption 5.1-6 can be generally satisfied in the PSAR-ANN models. White (p.747-748 [35]) also mentioned the condition  $E f_1^{1+\delta}(z;\boldsymbol{\theta}) < \infty$ . This condition on the domination function imposes a joint restriction on the probability measure which determines the data generating process and the network probability model to ensure the boundedness of the model. In our case, the network probability model is the logistic function and yields a bounded influence estimator with bounded  $\left| \frac{\partial^2}{\partial \boldsymbol{\theta}_j \partial \boldsymbol{\theta}_k} \ln f(z;\boldsymbol{\theta}) \right|$ ; then Assumption 5.7 is guaranteed to hold in a PSAR-ANN model.

**Lemma 2.** Given Assumptions 1-5,

$$\lim_{n \rightarrow \infty} \sup_{\boldsymbol{\theta} \in \Theta} \left| \frac{1}{n} \mathcal{L}_n(\boldsymbol{\theta}) - \mathcal{L}(\boldsymbol{\theta}) \right| \rightarrow 0 \quad a.s. \quad (8)$$

$\mathcal{L}(\boldsymbol{\theta})$  takes on the maximal value at  $\boldsymbol{\theta}_0$ .

*Proof.* The convergence result in (8) follows directly from Theorem 1 of Potscher and Prucha [25] if the following conditions hold:

- (1) The parameter space  $\Theta$  is compact.
- (2)  $l(\boldsymbol{\theta}|z)$  is equicontinuous on  $\Theta$ .
- (3)  $E f_1^{1+\delta}(z;\boldsymbol{\theta}) < \infty$  for some  $\delta > 0$ .
- (4) For each  $\boldsymbol{\theta} \in \Theta$ ,  $l(\boldsymbol{\theta}|z)$  satisfies the strong law of large numbers, i.e.  $\frac{1}{n} \mathcal{L}_n(\boldsymbol{\theta}) - \mathcal{L}(\boldsymbol{\theta}) \rightarrow 0 \quad a.s.$
- (5) There exists a monotone function  $h : [0, \infty) \rightarrow [0, \infty)$  with  $h(x) \rightarrow \infty$  as  $x \rightarrow \infty$  s.t.  $Eh(||z||) < \infty$

The condition (1) is a standard condition and satisfied by assumption 3.

The condition (2) is a special case of the smoothness condition mentioned in Potscher and

Prucha [25] when  $l(\boldsymbol{\theta}|z)$  is a single function but not a set of real functions; by assumption 5(6),  $l(\boldsymbol{\theta}|z) = \ln f(z; \boldsymbol{\theta}) + n^{-1} \ln |\mathbf{S}(\rho)|$  is equicontinuous on  $\mathbf{R} \times \boldsymbol{\Theta}$ .

The condition (3) can be satisfied in assumption 5(7).

The condition (4) is a necessary condition for uniform convergence. In our case,  $\{\varepsilon_s\}_{s=1}^n$  are independent and identically distributed with density  $f(\cdot)$ . The normal distribution, t distribution and the Laplace distribution have finite means and bounded covariances. This condition is also satisfied.

The condition (5) is a rather mild moment condition and one typical choice of function  $h$  is  $h(x) = x^p$ , where  $p > 0$  can be arbitrarily small (discussed in Potscher and Prucha p.676-677 [25]).

With all the five conditions satisfied, we can conclude the uniform convergence over a set  $\boldsymbol{\Theta}$  of parameter values. And Jensen's inequality implies that  $E(\ln l(\boldsymbol{\theta}|z))$  is uniquely maximized by  $\boldsymbol{\theta}_0$  for

$$E(\ln \frac{l(\boldsymbol{\theta}|z)}{l(\boldsymbol{\theta}_0|z)}) < \ln E(\frac{l(\boldsymbol{\theta}|z)}{l(\boldsymbol{\theta}_0|z)}) = 0 \quad \text{if } \boldsymbol{\theta} \neq \boldsymbol{\theta}_0$$

and so  $E(l(\boldsymbol{\theta}|z)) < E(l(\boldsymbol{\theta}_0|z))$  if  $\boldsymbol{\theta} \neq \boldsymbol{\theta}_0$ . In equation (8), as  $n \rightarrow \infty$ ,  $\mathcal{L}(\boldsymbol{\theta})$  is uniquely maximized at  $\boldsymbol{\theta}_0$ .  $\square$

We now give a formal statement of consistency results of the maximum likelihood estimator  $\hat{\boldsymbol{\theta}}_n$  based on the guideline in Potscher and Prucha (p.139 [26])

**Theorem 1.** Given Assumption 1-5,  $\hat{\boldsymbol{\theta}}_n - \boldsymbol{\theta}_0 \xrightarrow{a.s.} 0$  as  $n \rightarrow \infty$ .

*Proof.* Following White [34] Theorem 3.5 and Potscher and Prucha [26] Lemma 3.1,  $\hat{\boldsymbol{\theta}}_n - \boldsymbol{\theta}_0 \xrightarrow{a.s.} 0$  if the following conditions hold:

- (1) The parameter space  $\boldsymbol{\Theta}$  is compact.
- (2)  $n^{-1} \sum_{s \in \mathcal{S}} l(\boldsymbol{\theta}|z_s)$  is continuous in  $\boldsymbol{\theta} \in \boldsymbol{\Theta}$  and is a measurable function of  $z_s$ ,  $s \in \mathcal{S}$ , for all  $\boldsymbol{\theta} \in \boldsymbol{\Theta}$ .

(3)  $\mathcal{L}(\boldsymbol{\theta})$  is continuous on  $\boldsymbol{\Theta}$  and has a unique maximum at  $\boldsymbol{\theta}_0$ .

$$(4) \lim_{n \rightarrow \infty} \sup_{\boldsymbol{\theta} \in \boldsymbol{\Theta}} \left| n^{-1} \sum_{s \in \mathcal{S}} l(\boldsymbol{\theta}|z_s) - E_{\boldsymbol{\theta}_0} l(\boldsymbol{\theta}|z_s) \right| = 0, a.s.$$

Assumptions 1-5 and Lemma 2 guarantee all these conditions. Thus  $\hat{\boldsymbol{\theta}}_n - \boldsymbol{\theta}_0 \xrightarrow{a.s.} 0$  as  $n \rightarrow \infty$ .  $\square$

### 5.3 Asymptotic Distribution

First we define matrices,

$$\begin{aligned} A(\boldsymbol{\theta}_0) &= E\left[-\frac{\partial^2 l(\boldsymbol{\theta}_0|z)}{\partial \boldsymbol{\theta} \partial \boldsymbol{\theta}'}\right] \\ B(\boldsymbol{\theta}_0) &= E\left[\frac{\partial l(\boldsymbol{\theta}_0|z)}{\partial \boldsymbol{\theta}} \frac{\partial l(\boldsymbol{\theta}_0|z)}{\partial \boldsymbol{\theta}'}\right] \end{aligned} \quad (9)$$

and to construct asymptotic distributions of the maximum likelihood estimator, we also need the following assumption,

**Assumption 6.** (a)  $A(\boldsymbol{\theta}_0)$  is nonsingular; (b)  $B(\boldsymbol{\theta}_0)$  is bounded and nonsingular;

This assumption holds under fairly general conditions on data generating process and the neural network model (see White Appendix 3 [34]). We can conclude the asymptotic normality of the maximum likelihood estimator  $\hat{\boldsymbol{\theta}}_n$  as follows.

**Theorem 2.** Under Assumptions 1-6,

$$n^{1/2}(\hat{\boldsymbol{\theta}}_n - \boldsymbol{\theta}_0) \xrightarrow{d} N(\mathbf{0}, \boldsymbol{\Omega}_0) \quad (10)$$

where  $\boldsymbol{\Omega}_0 = A(\boldsymbol{\theta}_0)^{-1} B(\boldsymbol{\theta}_0) A(\boldsymbol{\theta}_0)^{-1} = A(\boldsymbol{\theta}_0)^{-1}$

*Proof.* See the Theorem 19.11 in White (p.748 [35]).  $\square$

Thus when the sample size  $n$  is sufficiently large, the probabilistic behavior of the parameter estimate  $\hat{\boldsymbol{\theta}}_n$  is described approximately normal with mean  $\boldsymbol{\theta}_0$ .

## 6 Numerical Results

### 6.1 Simulation Study

In this section, we conduct simulation experiments to examine the estimators' behavior for finite samples. The model used in our simulation is

$$y_s = \rho \sum_{i=1}^n w_{si} y_i + \lambda F(\gamma_1(x_s - \gamma_0)) + \varepsilon_s \quad (11)$$

For identification reasons, we impose the parameter  $\lambda > 0$  and  $\gamma_1 > 0$ .

We sample  $n = 2500, 4900$  random errors respectively from three distributions (standard normal, t-distribution and Laplace distribution) with variance 1 and  $x$  is a univariate exogenous variable sampled from a normal distribution  $N(0.5, 9)$ . Suppose the true parameters are  $\rho = 0.6$ ,  $\lambda = 5$ , and

## 6.1 Simulation Study

---

weights in the neural net  $\gamma_0 = 0.5$ ,  $\gamma_1 = 1$ . The log-likelihood function  $\mathcal{L}_n(\boldsymbol{\theta})$  is given in equation (6) and the maximization of the function  $\mathcal{L}_n(\boldsymbol{\theta})$  is through a searching procedure.

To measure the behavior of the estimators, the covariance of the asymptotic normal distribution can be calculated using equations in (9). Since matrices  $A$  and  $B$  in involve in calculating expected values, given merely observations, they can be estimated as follows:

$$\hat{A} = \frac{1}{n} \sum_{s=1}^n -\frac{\partial^2 l(\hat{\boldsymbol{\theta}}|z_s)}{\partial \boldsymbol{\theta} \partial \boldsymbol{\theta}'}$$

$$\hat{B} = \frac{1}{n} \sum_{s=1}^n \frac{\partial l(\hat{\boldsymbol{\theta}}|z_s)}{\partial \boldsymbol{\theta}} \frac{\partial l(\hat{\boldsymbol{\theta}}|z_s)}{\partial \boldsymbol{\theta}'}$$

where,

$$l(\boldsymbol{\theta}|z_s) = \frac{1}{n} \ln |\mathbf{S}(\rho)| - \frac{1}{2} \left\{ y_s - \rho \sum_{i=1}^n w_{si} y_i - \lambda F(\gamma_1(x_s - \gamma_0)) \right\}^2$$

To calculate  $\hat{A}$ , the second order derivatives are,

$$\frac{\partial^2 l(\boldsymbol{\theta})}{\partial \lambda \partial \rho} = - \left( \sum_{i=1}^n w_{si} y_i \right) F(\gamma_1(x_s - \gamma_0))$$

$$\frac{\partial^2 l(\boldsymbol{\theta})}{\partial \lambda \partial \lambda} = -F^2(\gamma_1(x_s - \gamma_0))$$

$$\frac{\partial^2 l(\boldsymbol{\theta})}{\partial \lambda \partial \gamma_1} = -\lambda(x_s - \gamma_0) F(\gamma_1(x_s - \gamma_0)) F'(\gamma_1(x_s - \gamma_0)) + \varepsilon_s(x_s - \gamma_0) F'(\gamma_1(x_s - \gamma_0))$$

$$\frac{\partial^2 l(\boldsymbol{\theta})}{\partial \lambda \partial \gamma_0} = \lambda \gamma_1 F(\gamma_1(x_s - \gamma_0)) F'(\gamma_1(x_s - \gamma_0)) - \varepsilon_s \gamma_1 F'(\gamma_1(x_s - \gamma_0))$$

$$\frac{\partial^2 l(\boldsymbol{\theta})}{\partial \gamma_1 \partial \rho} = -\lambda(x_s - \gamma_0) \left( \sum_{i=1}^n w_{si} y_i \right) F'(\gamma_1(x_s - \gamma_0))$$

$$\frac{\partial^2 l(\boldsymbol{\theta})}{\partial \gamma_1 \partial \gamma_1} = -\lambda^2(x_s - \gamma_0)^2 F'^2(\gamma_1(x_s - \gamma_0)) + \lambda \varepsilon_s(x_s - \gamma_0)^2 F''(\gamma_1(x_s - \gamma_0))$$

$$\frac{\partial^2 l(\boldsymbol{\theta})}{\partial \gamma_1 \partial \gamma_0} = -\lambda \varepsilon_s \{ F'(\gamma_1(x_s - \gamma_0)) + \gamma_1(x_s - \gamma_0) F''(\gamma_1(x_s - \gamma_0)) \}$$

$$+ \lambda^2 \gamma_1(x_s - \gamma_0) F'^2(\gamma_1(x_s - \gamma_0))$$

$$\frac{\partial^2 l(\boldsymbol{\theta})}{\partial \gamma_0 \partial \rho} = \lambda \gamma_1 \left( \sum_{i=1}^n w_{si} y_i \right) F'(\gamma_1(x_s - \gamma_0))$$

$$\frac{\partial^2 l(\boldsymbol{\theta})}{\partial \gamma_0 \partial \gamma_0} = \lambda \gamma_1^2 \varepsilon_s F''(\gamma_1(x_s - \gamma_0)) - \lambda^2 \gamma_1^2 F'^2(\gamma_1(x_s - \gamma_0))$$

where,

$$\varepsilon_s(\boldsymbol{\theta}) = y_s - \rho \sum_{i=1}^n w_{si} y_i - \lambda F(\gamma_1(x_s - \gamma_0))$$

To calculate  $\hat{B}$ , the first derivatives can be derived as follows:

$$\begin{aligned}\frac{\partial l(\boldsymbol{\theta})}{\partial \lambda} &= \{y_s - \rho \sum_{i=1}^n w_{si} y_i - \lambda F(\gamma_1(x_s - \gamma_0)) \cdot F(\gamma_1(x_s - \gamma_0))\} \\ \frac{\partial l(\boldsymbol{\theta})}{\partial \gamma_1} &= \{y_s - \rho \sum_{i=1}^n w_{si} y_i - \lambda F(\gamma_1(x_s - \gamma_0)) \cdot \lambda(x_s - \gamma_0) F'(\gamma_1(x_s - \gamma_0))\} \\ \frac{\partial l(\boldsymbol{\theta})}{\partial \gamma_0} &= -\{y_s - \rho \sum_{i=1}^n w_{si} y_i - \lambda F(\gamma_1(x_s - \gamma_0)) \cdot \lambda \gamma_1 F'(\gamma_1(x_s - \gamma_0))\}\end{aligned}$$

Note that the derivative of the log-likelihood with respect to  $\rho$  cannot be calculated directly because it requires taking derivative with respect to a log-determinant of a matrix  $\mathbf{I} - \rho \mathbf{W}$ . For small sample sizes, we can compute the determinant directly and get the corresponding derivatives; but for large sample sizes, for example a dataset with 3000 observations,  $\mathbf{W}$  is a  $3000 \times 3000$  weight matrix which makes it impossible to calculate the derivative directly. Since  $\mathbf{W}$  is symmetric, we can apply the spectral decomposition such that  $\mathbf{W}$  can be expressed in terms of its  $n$  eigenvalue-eigenvector pairs  $(\tau_i, \mathbf{v}_i)$ , where  $\tau_i, \mathbf{v}_i$  are the  $i$ th eigenvalue-eigenvector pair of  $\mathbf{W}$ .

$$\mathbf{W} = \sum_{i=1}^n \tau_i \mathbf{v}_i \mathbf{v}_i' = P \Lambda P'$$

Here let normalized eigenvectors  $\mathbf{v}_i$  be the column of a matrix  $P = [\mathbf{v}_1, \mathbf{v}_2, \dots, \mathbf{v}_n]$  and  $\Lambda$  is a diagonal matrix with eigenvalues  $\tau_i$  on its diagonal. Since  $\mathbf{v}_i$  are normalized,  $PP' = P'P = \mathbf{I}$ . Therefore, we can apply the following approach to calculate the derivative of  $\ln |\mathbf{I} - \rho \mathbf{W}|$ , which greatly reduce the burden of computations (Viton [33]).

$$\ln |\mathbf{I} - \rho \mathbf{W}| = \ln \left( \prod_{s=1}^n (1 - \rho \tau_i) \right)$$

Further we can compute the derivative of the log-likelihood function with respect to  $\rho$ .

$$\begin{aligned}\frac{\partial l(\boldsymbol{\theta})}{\partial \rho} &= \frac{\partial \prod_{s=1}^n (1 - \rho \tau_i)}{\partial \rho} \frac{1}{\prod_{s=1}^n (1 - \rho \tau_i)} + \{y_s - \rho \sum_{i=1}^n w_{si} y_i - \lambda F(\gamma_1(x_s - \gamma_0)) \cdot \left( \sum_{i=1}^n w_{si} y_i \right)\} \\ \frac{\partial^2 l(\boldsymbol{\theta})}{\partial \rho \partial \rho} &= \frac{1}{n} \frac{\partial^2 \prod_{s=1}^n (1 - \rho \tau_i)}{\partial^2 \rho} \frac{1}{\prod_{s=1}^n (1 - \rho \tau_i)} - \frac{1}{n} \left( \frac{\partial \prod_{s=1}^n (1 - \rho \tau_i)}{\partial \rho} \frac{1}{\prod_{s=1}^n (1 - \rho \tau_i)} \right)^2 - \left( \sum_{i=1}^n w_{si} y_i \right)^2\end{aligned}$$

Finally we can estimate the covariance matrix by equation (12).

$$\hat{\boldsymbol{\Omega}} = \hat{A}^{-1} \hat{B} \hat{A}^{-1} \tag{12}$$

In our simulation study, the mean and variance for  $\hat{\boldsymbol{\theta}}$  is calculated from 200 replicates. The asymptotic covariance matrix  $\hat{\boldsymbol{\Omega}}$  is computed based on a sample with 10000 simulated observations. From the Table 1, the empirical standard deviations are close to the asymptotic standard deviations which implies that the estimators' finite sample behavior matches their asymptotic distributions. Note that when  $\varepsilon$  is sampled from a Laplace distribution, this covariance matrix cannot be com-

## 6.2 Real Data Example

---

puted due to its second order derivative not differentiable. But the simulation results still exhibit normal properties. The QQ plots for parameter estimates are shown in Figure 4 and gives a strong indication of normality.

$\varepsilon$	$n = 2500$			
	$\hat{\rho}$	$\hat{\lambda}$	$\hat{\gamma}_0$	$\hat{\gamma}_1$
$N(0, 1)$	0.6178 (0.0075) [0.0046]	4.8504 (0.0812) [0.0639]	0.5410 (0.0425) [0.0417]	1.0576 (0.0431) [0.0354]
	0.6132 (0.0060) [0.0044]	4.8952 (0.0623) [0.0562]	0.5326 (0.0364) [0.0353]	1.0411 (0.0320) [0.0310]
	$Laplace$ $(0, \frac{\sqrt{2}}{2})$	0.6107 (0.0053)	4.9132 (0.0562)	0.5283 (0.0295)
$\varepsilon$	$n = 4900$			
	$\hat{\rho}$	$\hat{\lambda}$	$\hat{\gamma}_0$	$\hat{\gamma}_1$
$N(0, 1)$	0.6175 (0.0056) [0.0033]	4.8617 (0.0572) [0.0456]	0.5435 (0.0297) [0.0298]	1.0517 (0.0303) [0.0252]
	0.6130 (0.0051) [0.0031]	4.8957 (0.0526) [0.0426]	0.5312 (0.0274) [0.0260]	1.0380 (0.0246) [0.0235]
	$Laplace$ $(0, \frac{\sqrt{2}}{2})$	0.6096 (0.0047)	4.9242 (0.0487)	0.5217 (0.0239)

**Table 1:** Empirical mean and standard errors (in parentheses) of parameter estimates when  $\varepsilon$  is sampled from a standard normal, standardized student t distribution and a Laplace distribution. The asymptotic standard errors are displayed for reference in square brackets.

## 6.2 Real Data Example

### 6.2.1 Soil-water Tension in Iowa

Spatial models have lots of applications in environmental studies. For example, researchers and farmers who are interested in crop growth care about physical properties of soil within a field because these variations may be sizable and can affect plant growth and yield. And correctly understanding the crop yield may affect farmers' income from a business perspective. So soil-

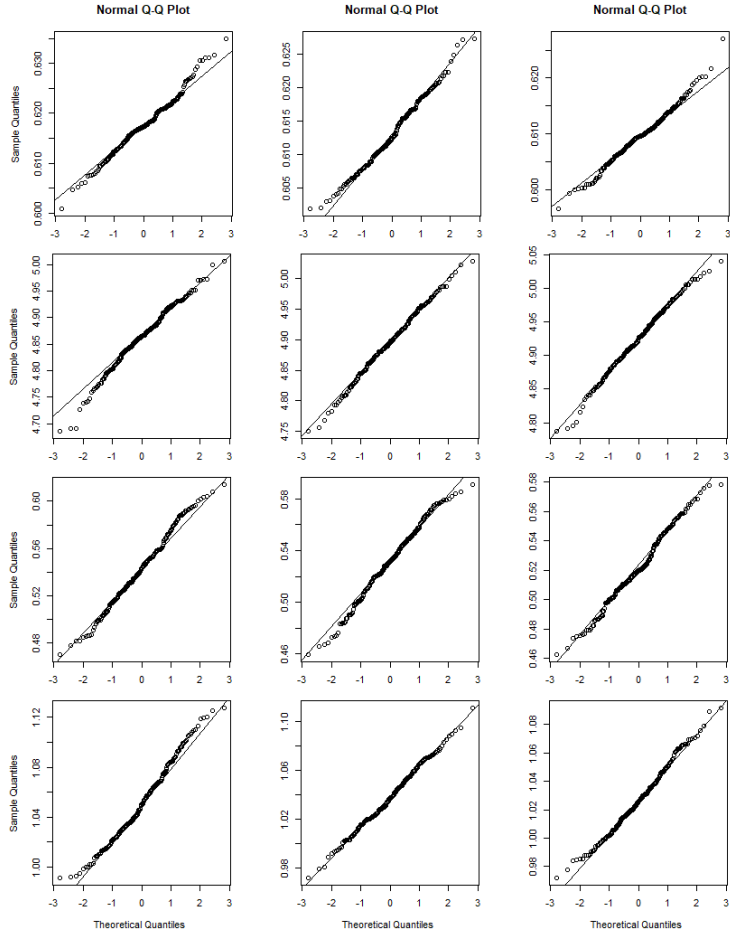


**Figure 4:** QQ-plots for parameter estimates  $\rho$  (1st row),  $\lambda$  (2nd row),  $\gamma_0$  (3rd row) and  $\gamma_1$  (4th row) when  $\varepsilon_s$  follows a standard normal distribution (first column), standardized t distribution (middle column) and Laplace distribution (last column)  $n = 70 \times 70$

physics data are important.

Classical statistical techniques are based on the assumption that observations are independent regardless of their distributions in space. Past studies (e.g., Campbell [8]; Burgess and Webster [6]; Russo and Bresler [29]; Vieira *et al.* [32]; Burrough [7]) are evidence that taking the spatial dependence into account can give a more complete understanding of phenomena influencing crop growth and yield under various tillage systems and configurations. A useful approach is to model physical measurements in a system with spatial relationships between them.

Therefore, we apply our PSAR-ANN model to soil-water tension data [9] collected during the 1983 crop season for the June to October period near Ames, in central Iowa. The data were recorded using tensiometers placed at 0.15m depths within the crop row. A grid network (Figure

## 6.2 Real Data Example

5), consisting of three rows by eight columns with spacing of 1.5 m between rows and 3 m between columns, was built on each plot to allow a spatial analysis. Tensiometer readings were made every two or three days. We use measurements on June 16th as our target variable  $y$  and measurements on June 15th as our explanatory variable  $x$ . The following 3D plot in Figure 5 is an overview of readings on June 16th.

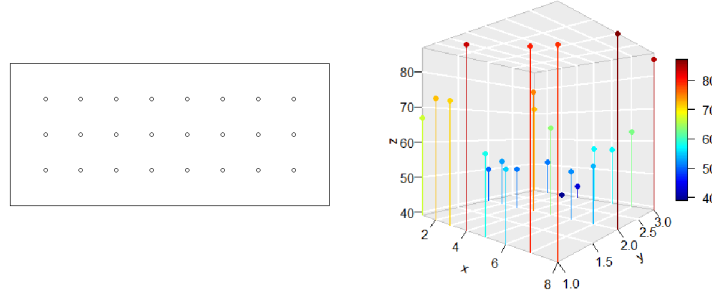


**Figure 5:** Locations for 24 measured plots (left) and a 3D view (right) of Measured Values of Soil-Water Tension at the 0.15 m Depth on June 16th

Through the spread of the color, we can observe that similar color points tend to be clustered in their neighborhood so it is reasonable to consider a spatial model for this example. We also make

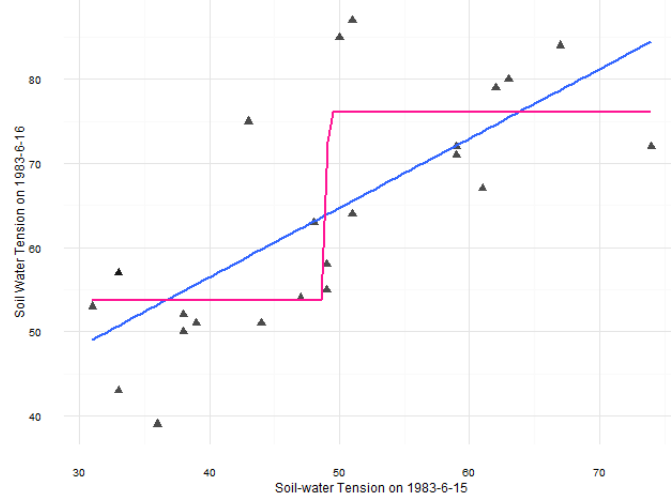


**Figure 6:** Measured Values of Soil-Water Tension at the 0.15 m Depth: the blue line is the linear regression fit and the red line is a logistic regression line

a scatter plot (Figure 6) of our data. The linear regression line ( $y = 23.53 + 0.8241x$ ) shown in the figure does not fit the data quite well with  $R^2 = 0.5216$  and Adjusted- $R^2 = 0.4998$ . However, a logistic function ( $y = 53.75 + 22.35 \cdot (1 + e^{-28.42 \cdot (x-49.07)})^{-1}$ ) fits better with  $R^2 = 0.6530$ . We assume the error follows a standard normal distribution and apply a PSAR-ANN model to the

data. The estimated model is

$$y_s = 0.89 \cdot \sum_{i=1}^{24} w_{si} y_i + 19.24 \cdot (1 + e^{-34.6 \cdot (x_s - 49.42)})^{-1} + \varepsilon_s \quad (13)$$

For the fitted model, the asymptotic standard deviations of the parameter estimates for  $(\rho, \lambda, \gamma_0, \gamma_1)^t$  are  $(0.0253, 2.4823, 0.0953, 6.3467)^t$  so all parameters are significant at 0.05 significance level.

The spatial correlation among plots is estimated to be  $\hat{\rho} = 0.89$ , showing a strong space dependence in the soil-water tension. This strong correlation indicates the fact that physical measurements in the field system do affect each other spatially. Taking this dependence into consideration in modeling can help us make better prediction in agricultural growth and business gain. The parameter  $\hat{\gamma}_0 = 49.42$  and the mean value of measurements on June 15th is 48.25. The estimated parameter  $\hat{\gamma}_0$  is close to the mean of  $x$  so we can treat  $\gamma_0$  here as a normalizing parameter.  $\hat{\lambda} = 19.24$  measures the effect of the logistic function with explanatory variables embedded.

The AIC of this PSAR-ANN model is 32.66, better than the linear model (AIC = 45.40) and classical spatial autoregressive model (AIC = 38.40). Therefore, the model appears to provide a better fit for the data when we include nonlinearity.

### 6.2.2 Violent Crimes in Chicago

In another example we look at violent crimes and foreclosures in the city of Chicago. Sociologists have identified a link between neighborhood characteristics and the geographical distribution of crimes. With the number of foreclosures increasing, recent literature [27] has documented the existence of a positive correlation between foreclosures and crime such as robbery and burglary. The rising violence leads to insecurity of the neighboring region and would negatively impact the economy in the long term. So to investigate this problem from a statistical perspective, we would like to take the geographical factor into consideration and use the proposed PSAR-ANN model to learn the link between violence crimes and foreclosures in the city of Chicago.

The data used here is public: the crime data as well as tracts shapefiles is collected through Chicago Data Portal and foreclosures data comes from the U.S. Department of Housing and Urban Development (HUD)[4]. The city of Chicago is divided into 897 smaller regions so the data has 897 observations. Our variable of interest is the number of violent crimes reported from January 2007 to December 2008 and the independent variable is the number of foreclosures divided by number of

## 6.2 Real Data Example

mortgages from January 2007 through December 2008. Both of them are nonnegative variables so allow zero inputs. In Figure 7, the original histogram (first graph) of the number of violent crimes is

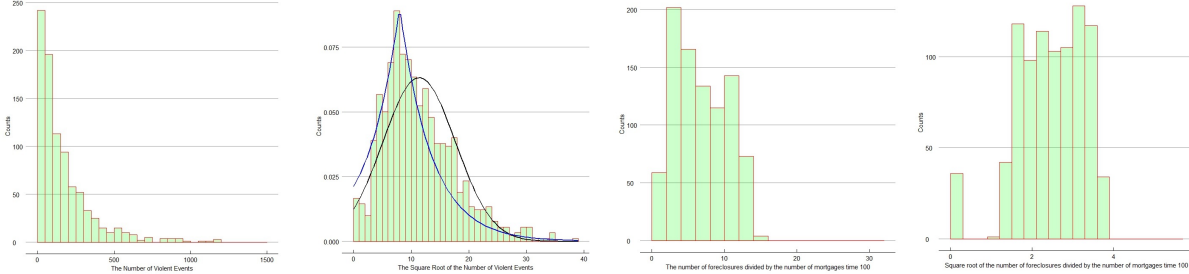


**Figure 7:** histogram of the number of violent crimes (upper left) and the square root of the number of violent crimes (upper right) in the city of Chicago; histogram of  $\frac{\text{number of foreclosures}}{\text{number of mortgages}} \times 100$  (lower left) and the square root of  $\frac{\text{number of foreclosures}}{\text{number of mortgages}} \times 100$  (lower right) in the city of Chicago;

highly skewed and has lots of zero observations. In order to stabilize the data and to fit into model assumptions, we use the square root transformation to stabilize this variable. The transformed variable looks more symmetric and we could use common distributions to model it such as normal distribution or Laplace distribution. Similar technique is applied to the explanatory variable (see the third and fourth graph in Figure 7). In the following analysis, we use the transformed data as  $y$  and  $x$ .

A linear regression model in this example is not appropriate because the observations are not independent violating the assumptions in the linear regression. The Global Moran's I test statistic standard deviate is 11.774 for the linear regression residual. P-value is smaller than 0.05 rejecting the hypothesis that there is no spatial correlation in observations. So a spatial model is a reasonable approach to solve this problem.

As mentioned before, to determine the distribution of  $\varepsilon$ , we can look into the histogram of observations. In Figure 7, the second plot represents the transformed target variable  $y$ . The black line is a normal density with  $\mu = \bar{y}$  and  $\sigma = s_y$  while the blue line is a corresponding Laplace density with  $\mu = \bar{y}$  and  $b = s_y/\sqrt{2}$ . Comparing the two densities, we find that a Laplace density is a better fit for the distribution of the error term  $\varepsilon$ . And through calculation, the approximate scale parameter for this Laplace density is  $b = 3$  so to fit into our model assumption, we scale the response variable  $y$  to have a unit variance. Based on the analysis of distribution of  $y$ , a PSAR-ANN

## 6.2 Real Data Example

---

model and its corresponding log-likelihood function are formulated as below.

$$y_s = \rho \sum_{s=1}^n w_{si} y_i + \lambda(1 + e^{-\gamma_1(x_s - \gamma_0)})^{-1} + \varepsilon_s$$

$$\mathcal{L}_n(\boldsymbol{\theta}) \propto \ln |\mathbf{I} - \rho \mathbf{W}| - \sqrt{2} \sum_{s=1}^n |\varepsilon_s|$$

where  $\boldsymbol{\theta} = (\rho, \lambda, \gamma_0, \gamma_1)'$ .  $\mathbf{W}$  is the weight matrix derived from the geographical information using the queen criteria and  $w_{si}$  is the  $(s, i)$  entry in this weight matrix. Through maximizing the log-likelihood function, the parameter estimates are  $\hat{\boldsymbol{\theta}} = (0.7021, 6.1916, 2.4857, 1.5570)'$ . And

$$y_s = 0.7021 \sum_{s=1}^n w_{si} y_i + 6.1916 \cdot (1 + e^{-1.5570 \cdot (x_s - 2.4857)})^{-1} + \varepsilon_s$$

The empirical standard deviations of parameter estimates are 0.03039, 1.8301, 0.4392, 0.5784 respectively so all parameters are significant at 0.05 significance level. The spatial correlation  $\rho$  is estimated to be 0.7021 indicating a strong positive correlation around the spatial neighborhood.  $\hat{\lambda} = 6.1916$  implies a positive correlation between the foreclosures and violent crimes supporting the conjecture of economists that the increasing number of foreclosures would lead to more violent crimes. More importantly the occurrence of violence in one location is strong dependent on that of its nearby communities.

To assess the model feasibility, the residual  $\varepsilon_s = y_s - \hat{y}_s$  is approximately Laplace distribution (see the Figure 8 below) so our model assumption seems reasonable.

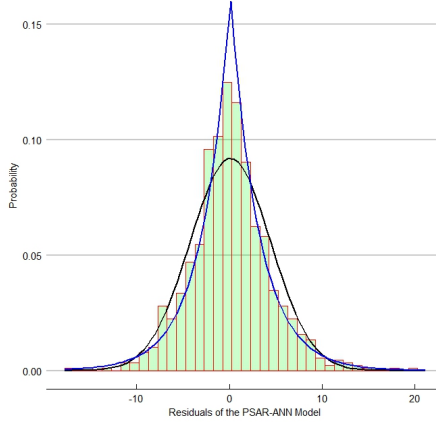


**Figure 8:** histogram of residuals under the fitted PSAR-ANN model: the black line is a normal density  $N(0, 1)$  and the blue line is a Laplace density  $Laplace(0, \frac{\sqrt{2}}{2})$

We also use Moran's I test on the model residuals and the P-value is 1 indicating that our model nicely eliminated the spatial correlations in the observations. A comparison of the original observations and residuals is in Figure 9.

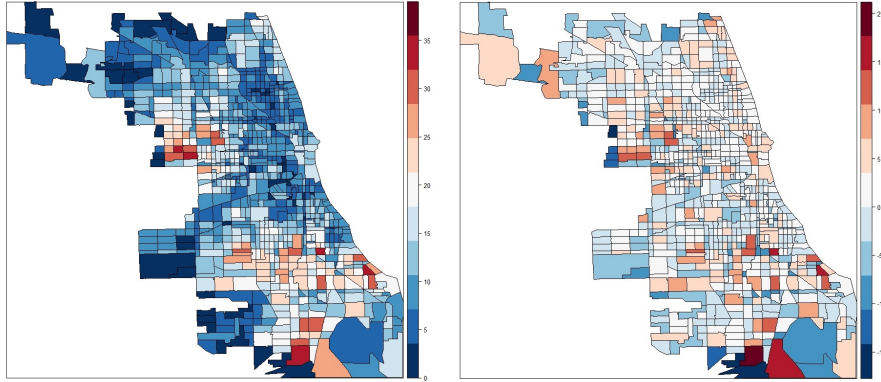


**Figure 9:** Regional heat maps of  $\sqrt{\text{the number of violent crimes}}$  (left) and PSAR-ANN model residuals (right)

## References

- [1] Chunrong Ai and Xiaohong Chen. Efficient estimation of models with conditional moment restrictions containing unknown functions. *Econometrica*, 71(6):1795–1843, 2003.
- [2] Beth Andrews, Richard A Davis, and F Jay Breidt. Maximum likelihood estimation for all-pass time series models. *Journal of Multivariate Analysis*, 97(7):1638–1659, 2006.
- [3] Luc Anselin. *Spatial econometrics: methods and models*, volume 4. Springer Science & Business Media, 2013.
- [4] Ignacio Sarmiento Barbieri. An introduction to spatial econometrics in r, 2017. URL <http://ignaciomsarmiento.github.io/2017/02/07/An-Introduction-to-Spatial-Econometrics-in-R.html>. [Online; accessed 10-Nov-2017].
- [5] F Jay Breid, Richard A Davis, Keh-Shin Lh, and Murray Rosenblatt. Maximum likelihood estimation for noncausal autoregressive processes. *Journal of Multivariate Analysis*, 36(2):175–198, 1991.
- [6] TMj Burgess and Richard Webster. Optimal interpolation and isarithmic mapping of soil properties. *European Journal of Soil Science*, 31(2):333–341, 1980.
- [7] PA Burrough. Multiscale sources of spatial variation in soil. i. the application of fractal concepts to nested levels of soil variation. *European Journal of Soil Science*, 34(3):577–597, 1983.
- [8] James B Campbell. Spatial variation of sand content and ph within single contiguous delineations of two soil mapping units. *Soil Science Society of America Journal*, 42(3):460–464, 1978.
- [9] Noel Cressie. *Statistics for spatial data*. John Wiley & Sons, 2015.
- [10] A Ronald Gallant and Halbert White. On learning the derivatives of an unknown mapping with multilayer feedforward networks. *Neural Networks*, 5(1):129–138, 1992.
- [11] Arthur Getis. Cliff, ad and ord, jk 1973: Spatial autocorrelation. london: Pion. *Progress in Human Geography*, 19(2):245–249, 1995.
- [12] Kurt Hornik, Maxwell Stinchcombe, and Halbert White. Universal approximation of an unknown mapping and its derivatives using multilayer feedforward networks. *Neural networks*, 3(5):551–560, 1990.

- [13] JT Gene Hwang and A Adam Ding. Prediction intervals for artificial neural networks. *Journal of the American Statistical Association*, 92(438):748–757, 1997.
- [14] Harry H Kelejian and Ingmar R Prucha. A generalized spatial two-stage least squares procedure for estimating a spatial autoregressive model with autoregressive disturbances. *The Journal of Real Estate Finance and Economics*, 17(1):99–121, 1998.
- [15] Harry H Kelejian and Ingmar R Prucha. A generalized moments estimator for the autoregressive parameter in a spatial model. *International economic review*, 40(2):509–533, 1999.
- [16] Harry H Kelejian and Ingmar R Prucha. Specification and estimation of spatial autoregressive models with autoregressive and heteroskedastic disturbances. *Journal of Econometrics*, 157(1):53–67, 2010.
- [17] Lung-Fei Lee. Asymptotic distributions of quasi-maximum likelihood estimators for spatial autoregressive models. *Econometrica*, 72(6):1899–1925, 2004.
- [18] J Pace LeSage et al. Introduction to spatial econometrics. Technical report, CRC Press, 2009.
- [19] James P LeSage et al. Spatial econometrics, 1999.
- [20] Keh-Shin Lii and Murray Rosenblatt. An approximate maximum likelihood estimation for non-gaussian non-minimum phase moving average processes. *Journal of Multivariate Analysis*, 43(2):272–299, 1992.
- [21] Marcelo C Medeiros, Timo Teräsvirta, and Gianluigi Rech. Building neural network models for time series: a statistical approach. *Journal of Forecasting*, 25(1):49–75, 2006.
- [22] WK Newey. Expository notes on uniform laws of large numbers. *Department of Economics, Princeton University*, 1987.
- [23] Keith Ord. Estimation methods for models of spatial interaction. *Journal of the American Statistical Association*, 70(349):120–126, 1975.
- [24] J Paelinck. Spatial econometrics. *Economics Letters*, 1(1):59–63, 1978.
- [25] Benedikt M Pötscher and Ingmar R Prucha. A uniform law of large numbers for dependent and heterogeneous data processes. *Econometrica: Journal of the Econometric Society*, pages 675–683, 1989.
- [26] Benedikt M Pötscher and Ingmar R Prucha. Basic structure of the asymptotic theory in dynamic nonlineaerco nometric models, part i: consistency and approximation concepts. *Econometric reviews*, 10(2):125–216, 1991.
- [27] FARHANA QAZI, APRIL L TROTTER, and JOEL HUNT. Looking for the link: The impact of foreclosures on neighborhood crime rates.
- [28] Thomas J Rothenberg. Identification in parametric models. *Econometrica: Journal of the Econometric Society*, pages 577–591, 1971.
- [29] David Russo and Eshel Bresler. Soil hydraulic properties as stochastic processes: I. an analysis of field spatial variability. *Soil Science Society of America Journal*, 45(4):682–687, 1981.
- [30] Oleg Smirnov and Luc Anselin. Fast maximum likelihood estimation of very large spatial autoregressive models: a characteristic polynomial approach. *Computational Statistics & Data Analysis*, 35(3):301–319, 2001.
- [31] Liangjun Su and Sainan Jin. Profile quasi-maximum likelihood estimation of partially linear spatial autoregressive models. *Journal of Econometrics*, 157(1):18–33, 2010.
- [32] Sidney Rosa Vieira, DR Nielsen, and JW Biggar. Spatial variability of field-measured infiltration rate. *Soil Science Society of America Journal*, 45(6):1040–1048, 1981.

- [33] Philip A Viton. Notes on spatial econometric models. *City and regional planning*, 870(03):9–10, 2010.
- [34] Halbert White. Parametric statistical estimation with artificial neural networks: A condensed discussion. *From statistics to neural networks: theory and pattern recognition applications*, 136:127, 1994.
- [35] Halbert White. *Estimation, inference and specification analysis*. Number 22. Cambridge university press, 1996.
- [36] Qiwei Yao, Peter J Brockwell, et al. Gaussian maximum likelihood estimation for arma models ii: spatial processes. *Bernoulli*, 12(3):403–429, 2006.
- [37] Yuan-qing Zhang and Guang-ren Yang. Statistical inference of partially specified spatial autoregressive model. *Acta Mathematicae Applicatae Sinica, English Series*, 31(1):1–16, 2015.